ACS APPLIED MATERIALS & INTERFACES

Research Article

www.acsami.org

Alternate Monolayers of CdSe Nanocrystals and Perylene Tetracarboxylate: Quantum Dot Hypersensitization for Dye-Sensitized Solar Cells

B. Vercelli and G. Zotti*

Istituto CNR per l' Energetica e le Interfasi, C.o Stati Uniti 4, 35127 Padova, Italy

A. Berlin

Istituto CNR di Scienze e Tecnologie Molecolari, via C. Golgi 19, 20133 Milano, Italy

Supporting Information

ABSTRACT: Mono- and multilayers from CdSe nanocrystal dispersion and perylene tetracarboxylate solution are reported for the first time. The layers were investigated by UV−visible spectroscopy, cyclic voltammetry, photoconductivity, and photoelectrochemical techniques. The n-type organic semiconductor gives enhanced photoconductivity to the CdSe-NC multilayer structure. The photoactive perylene monolayer acts also as hypersensitizer of CdSe-NC structures. The perylene-modified CdSe-NC monolayer on indium tin oxide (ITO) electrode in a three-electrode photoelectrochemical cell upon illumination in the presence of oxygen generates an intense steady photocurrent as high as 10−20 times that expected from the individual contributions of perylene and CdSe-NCs. The hypersensitization mechanism is discussed on the basis of the energy level diagram of the components.

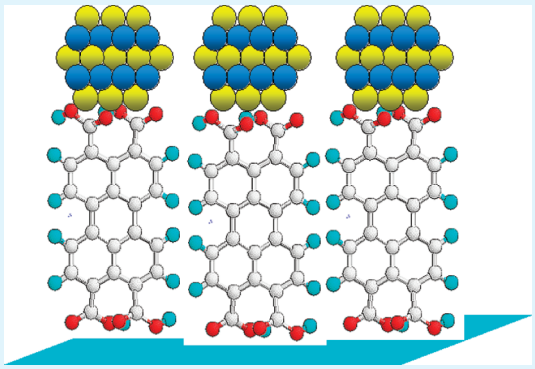

KEYWORDS: *solar cells, multilayers, hypersensitizer, photoelectrochemistry, photoconductivity, cyclic voltammetry, phototransport*

1. INTRODUCTION

Perylene and its derivatives are among the most attractive luminescence dyes[1] owing to their high quantum yields and good photochemical stability. They have been employed in various applications in electronics and optoelectronics including photovoltaics.[1]

Perylene tetracarboxylic acid derivatives, the energy gap of which is only 2.5 eV, have unique properties.[2−4] Such a small energy gap implies a semiconductor-like behavior and also redox activity.[5] Perylene derivatives show an n-type, electron conducting behavior and serve as electron-acceptor materials. Perylene 3,4,9,10-tetracarboxylic dianhydride[6] or diimide[7] are in fact n-type molecules[8] previously used in organic electronics. Due to their symmetrical and planar structure, the perylene molecules easily form aggregates through $\pi-\pi$ or dipole−dipole interactions. Crystal packing consists of dimers arranged in a herringbone fashion.[9]

Perylenes have found early applications in thin film organic solar cells in couple with phthalocyanine.[10] Studies performed before the mid 1980s showed very low power conversion efficiencies, but later (1986), a bilayer *pn*-heterojunction cell consisting of copper phthalocyanine and perylene between indium tin oxide (ITO) and Ag electrodes gave a noticeable (ca. 1%) power conversion efficiency.[10] Extensive studies have since been performed on such photovoltaic devices, resulting in significant improvements in the power conversion efficiency. The photoconductive properties of a bilayer photodiode with two organic thin films, composed of poly(3-butylthiophene) and a perylene diimide derivative sandwiched between two electrodes have been demonstrated.[11] Perylene, as tetracarboxydiimide, is actually a very common electron acceptor, used in couple with a conjugated polymer, such as oligo(fluorene-*alt*-bithiophene),[12] poly(3-hexylthiophene),[13,14] or polyphenylenevinylene,[15] as electron donors, in efficient organic solar cells. Quite recently, carbon nanotubes and cadmium selenide nanocrystals (CdSe-NCs) have been connected via a thiol-substituted perylene with improved photoconductivity.[16]

Perylene derivatives are also commonly used for dye-sensitized solar cells.[17] Perylene bis(dicarboximide) derivatives have also been arranged in multilayers on ITO substrate,[18,19] and perylene multilayers for photovoltaic applications have recently been reported.[20] Recently, sensitization of mesoporous TiO_2 photoelectrodes with cadmium selenide nanocrystals (CdSe-NCs)[21−24] has attracted much attention, and a combination of perylene and CdSe-NCs may give interesting developments. For this twin set, the literature reports

Received: April 4, 2012
Accepted: June 4, 2012
Published: June 4, 2012

 © 2012 American Chemical Society

nanostructures formed via self-assembly of ZnS-capped CdSe-NCs and perylene bis(dicarboximide) dyes[25] and the production of poly[perylene bis(dicarboximide)] doped with CdSe-NCs, with possibly improved photoelectric conversion efficiency.[26]

We recently investigated the enhancement of photoconduction in CdSe-NCs by n-type organic linkers.[27] In this report, we address the specific role in CdSe-NCs of perylene, as a well-known n-conductor, acting both as source and transport mediator of photogenerated electrons. We used the layer-by-layer (LBL) method to assemble on an ITO surface hybrid organic/CdSe multilayer thin films from nonaqueous solutions of bis(tetrabutylammonium) salt of perylene 3,4,9,10 tetracarboxylic acid (hereafter PerCA4) and CdSe-NCs (see Scheme 1, pictorial view of the first bilayer). Hexadecylamine/stearate-capped CdSe-NCs of 7.5 nm diameter were used to take advantage of the broad absorption of such relatively large NCs, over which the perylene absorption is easily discerned. The multilayer buildup was monitored by UV−vis spectroscopy, and the new materials were investigated by cyclic voltammetry, UV−vis and FTIR spectroscopy, photoelectrochemistry, and photoconductivity. The specific role of perylene tetracarboxylate as sensitizer has also been addressed and investigated mainly by photoelectrochemical techniques, also in comparison with a sexithiophene dicarboxylate (Chart 1).

Scheme 1. Pictorial View of a Bilayer of PerCA4 and CdSe-NCs

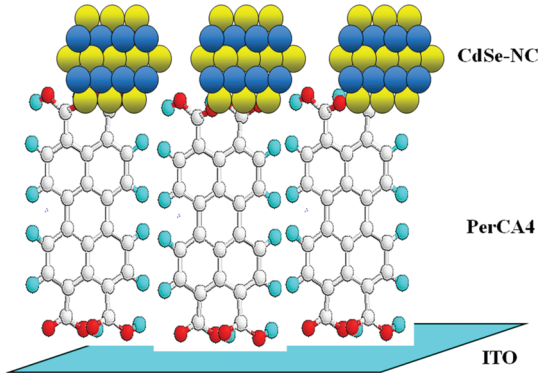

Chart 1

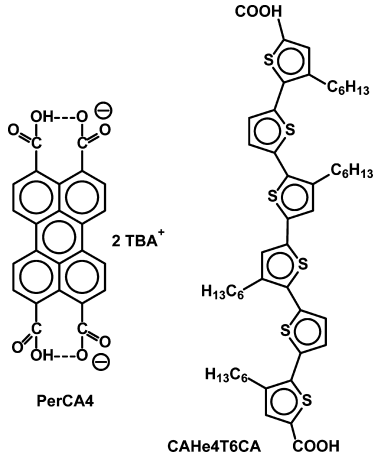

2. EXPERIMENTAL SECTION

2.1. Chemicals and Reagents. Acetonitrile was reagent grade (Uvasol, Merck) with a water content <0.01%. The supporting electrolytes, tetrabutylammonium perchlorate (TBAP) and $NaClO_4$, and all other chemicals used for characterizations were reagent grade and used as received. Poly(vinylbenzoic) acid (PVBH) was prepared as reported previously.[28]

The compound perylene 3,4,9,10-tetracarboxylic dianhydride was reagent grade from Aldrich. The relevant bis(tetrabutylammonium) salt (PerCA4) was prepared as described below and used ca. 10^{-3} M in EtOH. The 3,3‴,4‴,3⁗⁗-tetrahexyl-[2,2′;5′,2″;5″,2‴;5‴,2⁗;5⁗,2⁗⁗;5⁗⁗,2⁗⁗⁗]-sexithiophene-5,5⁗⁗⁗-dicarboxylic acid (CAHe4T6CA) was prepared as described in the literature[29] and used as the tetrabutylammonium salt 10^{-3} M in ethanol.

Soluble CdSe-NCs with the surface capped by hexadecylamine and stearic acid were produced as previously reported.[28] The NCs display the first exciton peak at 645 nm, corresponding to an average size of 7.5 nm.[30] Their highest occupied molecular orbital (HOMO) and lowest unoccupied molecular orbital (LUMO) values are located at −5.6 and −3.7 eV vs vacuum.[31] CdSe-NCs were used ca. 10^{-2} M (in CdSe units) in $CHCl_3$.

Synthesis of PerCA4. Tetrabutylammonium hydroxide (13 mg, 0.050 mmol) was added to a suspension of perylene 3,4,9,10-tetracarboxylic dianhydride (10 mg, 0.025 mmol) in ethanol (10 mL), and the reaction mixture was refluxed for 2 h. The solvent was evaporated at reduced pressure giving the title compound as an orange solid soluble in the common solvents such as ethanol, acetone, and acetonitrile.

IR (FTIR) ν_{max} 3300, 1715, 1600, 1490, 1350, 1270 cm^{-1} (Figure S1, Supporting Information); UV−vis (ethanol) λ_{max} 470 nm (Figure S2, Supporting Information); CV reduction (acetonitrile + 0.1 M TBAP) $E_1 = -1.91$ V, $E_2 = -2.24$ V (vs Ag/Ag^+). Further details are reported in Supporting Information.

2.2. Substrates and Multilayer Film Formation. Transparent conducting surfaces were prepared from indium tin oxide (ITO)-glass electrodes (20 Ω sq^{-1} from Kintec, Hong-Kong). The ITO-glass electrodes for CdSe-NC layering were first modified with PVBH 10^{-3} M in ethanol, as previously reported.[28] The build-up of multilayers was performed on the modified ITO-glass electrodes by the LBL methodology, i.e., by dipping the electrodes alternatively into the solutions of the CdSe-NC and linker. Exposure time was 5 min.

2.3. Apparatus and Procedure. *Electrochemistry, Spectroscopy, and Profilometry.* Experiments were performed at room temperature under nitrogen in three electrode cells in acetonitrile + 0.1 M TBAP or $NaClO_4$ as supporting electrolyte. The counter electrode was platinum; reference electrode was a silver/0.1 M silver perchlorate in acetonitrile (0.34 V vs SCE). The voltammetric apparatus (AMEL, Italy) included a 551 potentiostat modulated by a 568 programmable function generator. The working electrode for cyclic voltammetry was a platinum or glassy carbon minidisc electrode (0.003 and 0.06 cm^2 area, respectively). CV of multilayers was performed on 1 × 4 cm^2 ITO-glass samples with an exposed area of 1 cm^2 and at a scan rate of 0.02 V s^{-1}.

Electronic spectra were obtained from a Perkin-Elmer Lambda 15 spectrometer. Absorbance data are given as measured, i.e., for the sum of the ITO and glass sides, the same level of functionalization being obtained at both sides of the electrode.

FTIR spectra were taken on a Perkin-Elmer 2000 FTIR spectrometer. FTIR spectra of films were taken in reflection−absorption mode.

PL spectra were run at room temperature with a Xenon lamp monochromated at an excitation wavelength of 450 nm in 10 mm optical path quartz cuvettes. Multilayer thicknesses were determined with an Alphas-step IQ profilometer from KLA Tencor.

Photoelectrochemistry. Photoelectrochemical experiments were performed in O_2-saturated water (or acetonitrile) + 0.1 M $NaClO_4$ solutions, using a conventional three-electrode cell with a saturated calomel electrode (SCE) (or silver/0.1 M silver perchlorate in acetonitrile) as a reference and a platinum counter electrode. The

dx.doi.org/10.1021/am300590a | ACS Appl. Mater. Interfaces 2012, 4, 3233−3238

working electrode was illuminated on the solution side with a water-filtered 100 W halogen lamp, spotted over ca. 10 cm^2. The resulting light power, calibrated with a Si photodiode, was ca. 100 mW cm^{-2}. Light was chopped with a manually driven shutter.

Photoconductivity. Photoconductivity measurements of multilayers were performed with a special Hg electrode contacting the multilayer-covered ITO as described previously.[28] Bias was applied to ITO vs Hg electrode. Illumination (100 mW cm^{-2}) was performed as described above on the back glass side of the ITO/multilayer.

3. RESULTS AND DISCUSSION

3.1. PerCA4 Monolayer. PerCA4 (10^{-3} M solution in ethanol) forms on ITO a monolayer with maximum at 478 nm (2.6 eV) and absorbance of 8×10^{-3} (Figure S3, Supporting Information). From the extinction coefficient measured in ethanol solution, the coverage is 1×10^{-10} mol cm^{-2}. The spectrum corresponds essentially to that in solution, which suggests that no significant lateral interaction is operative among the adsorbed molecules. In the monolayer, two of the four carboxylic groups of PerCA4 molecule are bound to the solid surface; the other two groups are free and able to react further.[32]

PerCA4 as monolayer on ITO dissolves in water but is insoluble in acetonitrile, methylene chloride, and chloroform. In acetonitrile + 0.1 M $NaClO_4$, where it is stable, the monolayer is irreversibly reduced at $E_p = -1.73$ V and oxidized at $E_p = 0.77$ V (Figure S4, Supporting Information). The electrochemical gap (2.5 V) agrees nicely with the optical gap. The resulting energy diagram, compared with that of 7.5 nm CdSe-NCs, is shown in Scheme 2.

Scheme 2. Energy Diagram of CdSe-NCs, PerCA4, and CAHe4T6CA

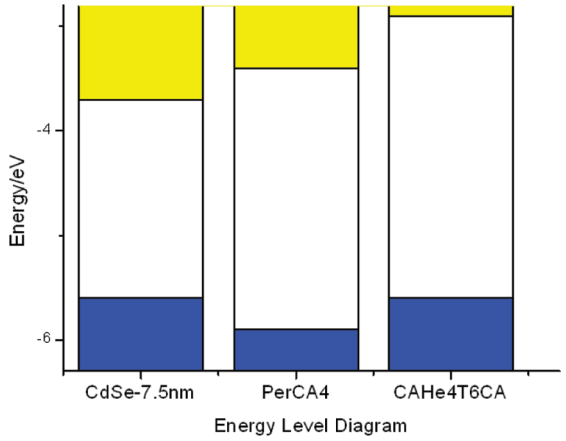

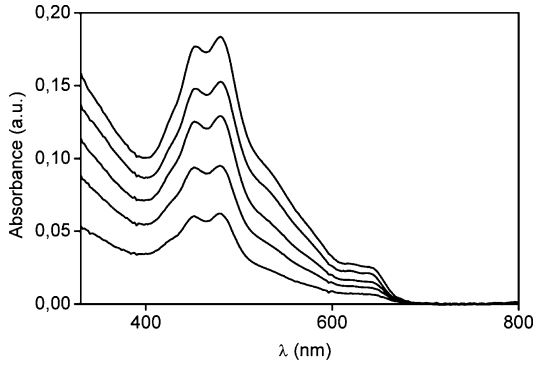

Figure 1. UV−vis spectra of ITO/$(CdSe/PerCA4)_n$ multilayers (n = 1−5). Spectra are background-corrected.

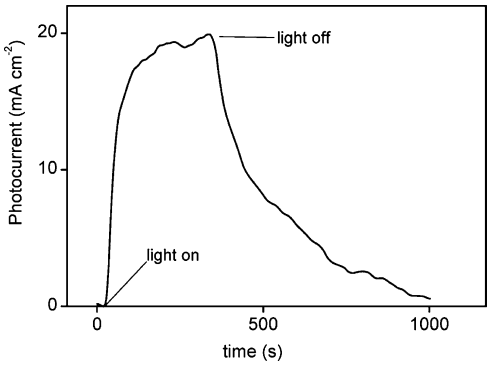

Figure 2. Photocurrent transients of ITO/CdSe/$(PerCA4/CdSe)_9$/Hg multilayer at 1 V applied voltage and 100 mW cm^{-2} illumination. Rise time (to 90%): 100 s; decay time: 500 s.

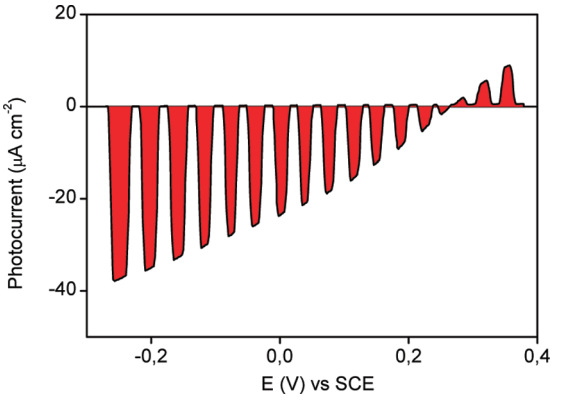

Figure 3. Photoelectrochemical i−V plots of ITO/CdSe/$(PerCA4/CdSe)_9$ multilayer in 0.1 M $NaClO_4$ under O_2 at 100 mW cm^{-2} illumination; scan rate: 0.05 V s^{-1}.

3.2. CdSe/PerCA4 Multilayers. Multilayers are built on PVBH-primed ITO via alternation of CdSe-NCs dispersion in chloroform and PerCA4 solution in ethanol. For clarity, the ITO/PVBH/CdSe-NC layer will be hereafter indicated as ITO/CdSe.

Electronic spectra of multilayers with progressive growth are shown in Figure 1. The optical differential growth is 5×10^{-3} au at 645 nm (CdSe-NC first exciton band) and 35×10^{-3} au at 470 nm (PerCA4, CdSe subtracted). Given a molar extinction coefficient of 1.2×10^6 $M^{-1}cm^{-1}$ for this size of the nanocrystals,[30] the CdSe-NC coverage is 2×10^{-12} nanocrystal mol cm^{-2} (1.2×10^{12} particles cm^{-2}). From its extinction coefficient, the PerCA4 coverage is ca. 4×10^{-10} mol cm^{-2} $layer^{-1}$, which corresponds to a dense coverage of the CdSe-NCs, ca. 4 times that of the first layer on ITO. This result is due to the higher roughness of the CdSe layer compared with the PVBH-primed ITO surface.

In such multilayers, we may note the presence of a strong shoulder at 540 nm. We attribute this shoulder, absent in solution spectra and small in the spectrum of the monolayer on ITO, to the forbidden transition to the lowest singlet dimer state. This transition becomes partially allowed in the disordered sample due to slight deviations from the parallel orientation of the molecular planes in the dimers.[33] Thus, PerCA4 in the dense monolayers is, at least partially, aggregated in dimers.

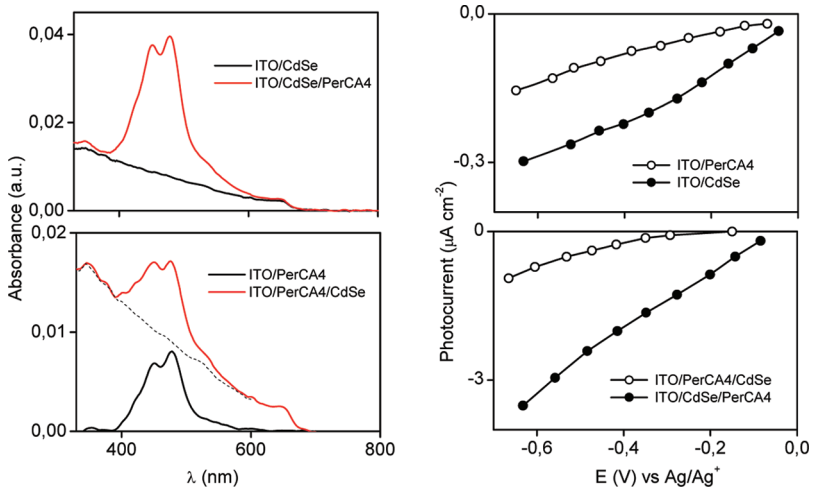

Figure 4. Left: UV−vis spectra of PerCA4 and CdSe monolayers and bilayers. Spectra are background-corrected. Right: Photoelectrochemical *i*−*V* plot for PerCA4 and CdSe monolayers and bilayers in acetonitrile + 0.1 M $NaClO_4$. Scan rate: 0.005 V s^{-1}.

Scheme 3. Energy Diagram of ITO, 7.5-nm CdSe-NCs, PerCA4, and O_2

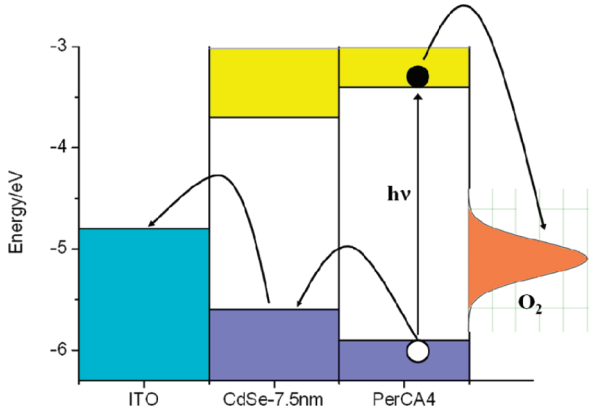

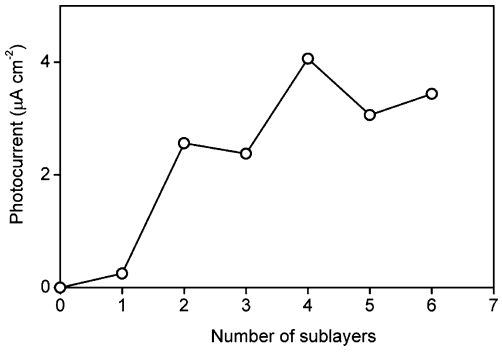

Figure 5. Photocurrent at −0.5 V of ITO/$(CdSe/PerCA4)_n$ multilayers in acetonitrile + 0.1 M $NaClO_4$ in progression of sublayers. Scan rate: 0.005 V s^{-1}.

Multilayers appear very uniform under SEM examination, although there is no apparent difference with bare ITO. In fact, the multilayers are thin if compared with the ITO grain size. Moreover, the multilayers are robust enough to stand a standard sticky-tape test with no appreciable loss. The $(CdSe/PerCA4)_{10}$ multilayer is 50 nm thick, in good agreement with the value expected from particle size and packing mode.[28]

3.3. Photoconductivity and Photoluminescence of Multilayers. The ITO/$(CdSe/PerCA4)_n$ multilayer displays an intense photocurrent at 1 V bias and 100 mW cm^{-2} illumination. A typical transient, shown in Figure 2, evidences a slow response time of several seconds. This is in fact a case of trap-induced photocurrents, in which the recombination lifetime is limited by the release rate of the trap, and this results in slow response times.[34]

The compact $(CdSe/PerCA4)_{10}$ multilayer provides a photocurrent of 20 mA cm^{-2}, which is among the strongest photocurrent responses we have measured in multilayers alternating CdSe-NCs and organic compounds.[28] As expected from the n-type conductivity of the perylene linkers,[6,7,35,36] no obstacle is practically interposed to transport photogenerated electrons, as recently shown for a series of n-type linkers in CdSe-NC multilayers.[27]

This result agrees with the enhanced photoconduction found in carbon nanotubes and CdSe-NCs after connection with thiol-substituted perylene.[16] In nanoassembled CdSe-NCs and perylene bisimide, CdSe photoluminescence is quenched.[25] On the other hand, a complete photoluminescence quenching is observed also in our CdSe/PerCA4 multilayers, which in principle favors charge transport.

3.4. Photoelectrochemistry. Photoelectrochemical behavior is important for applications in dye-sensitized solar cells (DSSCs). These typically operate as photoanodes, where photocurrents result from dye-sensitized electron injection into n-type semiconductors (generally TiO_2) and electrons are extracted from sacrificial species such as iodide[37,38] or sulfide.[39] Dye-sensitized photocathodes operate in an inverse mode, where dye-excitation is followed by rapid electron transfer from a p-type semiconductor (typically NiO) to the dye (dye-sensitized hole injection). In these cells, electrons are injected into the solution containing an electron scavenger. In the photoelectrochemical investigations described below, we have used dioxigen as electron scavenger.

Multilayers. A photoelectrochemical experiment ITO/$CdSe/(PerCA4/CdSe)_9$ multilayer in O_2-saturated aqueous 0.1 M $NaClO_4$ solution is shown in Figure 3 as a typical example. The electrode was illuminated on the solution side with chopped light from a halogen lamp. Light-induced O_2-reduction currents on a low background current were observed between −0.5 and 0.1 V vs SCE, with no mass transfer control. Losses or degradation are negligible as confirmed by

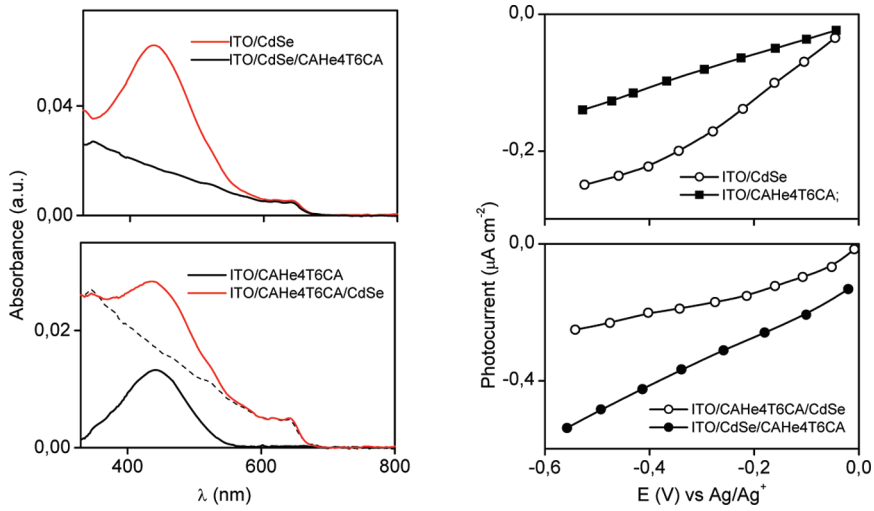

Figure 6. Left: UV−vis spectra of CdSe and CAHe4T6CA monolayers and bilayers (spectra are background-corrected). Right: Photoelectrochemical *i*−*V* plot for CdSe and CAHe4T6CA monolayers and bilayers in acetonitrile + 0.1 M $NaClO_4$. Scan rate: 0.005 V s^{-1}.

spectroscopic analysis before and after the photoelectrochemical experiment.

Oxygen photoreduction proceeds with a typical sublinear *i*−*V* curve, attaining a current of ca. 40 μA cm^{-2} at −0.3 V from an onset potential of ca. 0.3 V (vs SCE). The high photocurrent level, ca. twice that measured on analogous linker/CdSe multilayers,[27] may be associated with carrier generation also in the photoactive linker molecules. To clarify this point, investigations on CdSe and PerCA4 single monolayers and their bilayer combinations were performed, as reported in the following section.

Monolayers and Bilayers. This study was performed in O_2-saturated acetonitrile + 0.1 M $NaClO_4$, in the potential range from 0.0 V (photocurrent onset potential) to −0.7 V vs Ag/Ag^+, where the background current in the dark is negligible. In all cases, the *i*−*V* photocurrent responses of oxygen reduction in this medium are approximately linear with the applied potential.

Figure 4 shows the spectra of the ITO/PerCA4 and ITO/CdSe monolayers and of the ITO/PerCA4/CdSe and ITO/CdSe/PerCA4 bilayers. The CdSe monolayer has an absorbance of 5×10^{-3} au at the exciton energy of 645 nm. The ITO/PerCA4/CdSe bilayer is simply the sum of the two spectra, whereas the ITO/CdSe/PerCA4 bilayer shows the same CdSe contribution but a ca. 4-times higher contribution from adsorbed PerCA4 (see before).

As shown in Figure 4, at an applied voltage of −0.5 V, the responses are 0.1 and 0.25 μA cm^{-2} for the ITO/PerCA4 and ITO/CdSe monolayers. In the ITO/PerCA4/CdSe bilayer, the response is increased to ca. 0.5 μA cm^{-2}, as a rough sum of the two separate contributions, yet in the ITO/CdSe/PerCA4, the response is strongly increased by 10−20 times to ca. 2.5 μA cm^{-2}. This result cannot be attributed to the increased adsorption of PerCA in the bilayer solely, since the 4-fold adsorption increase, compared with the bare PerCA4 monolayer on ITO, would have increased the CdSe response from 0.25 to 0.7 μA cm^{-2} at most.

The impressive increase (enhanced sensitization or hypersensitization) can be accounted for by charge separation at the CdSe/PerCA4 interface. Considering the energy diagram in Scheme 3, it is clear that the electron−hole pair formed at the surface PerCA4 layer can be easily separated by hole transfer to the neighbor CdSe layer, given the difference of HOMO energy levels, therefore increasing the lifetime of the excited electron and consequently its O_2-reduction rate. Such a mechanism could in principle be corroborated by PL quenching experiments, but the PerCA4 monolayer is so low emissive as to prevent such test. From inspection of Scheme 3, it is clear that, in the inverted ITO/PerCA4/CdSe bilayer, such a mechanism is not energetically allowed. In this case, the electron−hole pair formed at the surface CdSe layer cannot be separated by hole transfer to the neighbor PerCA4 layer.

This mechanism may be operating and amplified in the LBL sequence. In the progression of sublayers, starting from the CdSe monolayer, the photocurrent has the progression shown in Figure 5, from which it is clear that hypersensitization given by the first PerCA4 sublayer is increased at the second sublayer, but with a further gain of 50% only. With subsequent layers, the photocurrent decreases due to increased resistance of the multilayer. We can thus conclude that hypersensitization by PerCA4 is practically effective at the first monolayer only.

To give support to the previous explanation of hypersensitization of CdSe-NCs by PerCA4, we have made a comparison with monolayers from CAHe4T6CA,[29] i.e., a sexithiophene absorbing at the same spectral region of PerCA4 (maximum at 441 nm, i.e., optical gap of 2.8 eV) but with a different disposition of the HOMO−LUMO levels (see energy diagram in Scheme 2), such as to inhibit hypersensitization. In fact, a CAHe4T6CA monolayer is reversibly oxidized at ca. −5.6 eV vs vacuum,[29] very close to that of the CdSe-NCs.

Figure 6 shows the spectra of the ITO/CAHe4T6CA and ITO/CdSe monolayers and of the ITO/CAHe4T6CA/CdSe and ITO/CdSe/CAHe4T6CA bilayers. The CAHe4T6CA monolayer shows a maximum absorbance of 13×10^{-3} au (the coverage is 1×10^{-10} mol cm^{-2}).[29] The spectrum of the ITO/CAHe4T6CA/CdSe bilayer is simply the sum of the two separate monolayer spectra, whereas the ITO/CdSe/CAHe4T6CA bilayer shows the same CdSe response but a ca. 3-times higher contribution from adsorbed CAHe4T6CA. The whole pattern is much the same observed as in the case of PerCA4.

As shown in Figure 6, at an applied voltage of −0.5 V, the responses are 0.15 and 0.25 μA cm^{-2} for the ITO/CAHe4T6CA and ITO/CdSe monolayers, respectively. In

the ITO/CAHe4T6CA/CdSe bilayer, the response is ca. 0.25 μA cm^{-2}, as in the CdSe monolayer. In the ITO/CdSe/CAHe4T6CA, the response is increased only to ca. 0.5 μA cm^{-2}, which is in any case lower than the sum (0.7 μA cm^{-2}) of the contributions from the CdSe and CAHe4T6CA sublayers. It is thus confirmed that no hypersensitization is operating in this case.

4. CONCLUSIONS

We have reported in detail the preparation and characterization of multilayers from perylene tetracarboxylate and CdSe-NCs. The n-type organic semiconductor gives enhanced photoconductivity to the CdSe-NC multilayer structure.

We report a photoactive perylene monolayer as hypersensitizer of CdSe-NC structures. UV−visible spectra and cyclic voltammetry showed that the monolayer has a densely packed structure. Photoelectrochemical measurements have shown that perylene gives enhanced sensitization (hypersensitization) to CdSe-NC modified ITO electrodes. The impressive (10−20 times) increase of photocurrent response may be useful for the production of dye-sensitized solar cells. Work is in progress to verify if power conversion efficiency of such DSSC is consequently improved.

■ ASSOCIATED CONTENT

Supporting Information

Characterization of PerCA4; FTIR spectra of perylene 3,4,9,10-tetracarboxylic dianhydride and PerCA4; UV−vis absorption and PL spectra of PerCA4 in ethanol solution; UV−vis spectrum and CV of PerCA4 monolayer on ITO. This material is available free of charge via the Internet at http://pubs.acs.org.

■ AUTHOR INFORMATION

Corresponding Author

*Tel: (+39)49-8295868. Fax: (+39)49-8295853. E-mail: g.zotti@ieni.cnr.it.

Notes

The authors declare no competing financial interest.

■ REFERENCES

(1) Liu, Y.; Yang, C.; Li, Y.; Wang, S.; Zhuang, J.; Liu, H.; Wang, N.; He, X.; Li, Y; Zhu, D. *Macromolecules* **2005**, *38*, 716−721.
(2) Gregg, B. A.; Cormier, R. A. *J. Am. Chem. Soc.* **2001**, *123*, 7959−7960.
(3) Thelakkat, M.; Schmitz, C.; Schmidt, H. W. *Adv. Mater.* **2002**, *14*, 577−581.
(4) Schmidt-Mende, L.; Fechtenkotter, A.; Mullen, K.; Moons, E.; Friend, R. H.; MacKenzie, J. D. *Science* **2001**, *293*, 1119−1122.
(5) Xu, B.; Xiao, X.; Yang, X.; Zang, L.; Tao, N. *J. Am. Chem. Soc.* **2005**, *127*, 2386−2387.
(6) Laquindanum, J .G.; Katz, H. E.; Dodabalapur, A.; Lovinger, A. J. *J. Am. Chem. Soc.* **1996**, *118*, 11331−11332.
(7) Malenfant, P. R. L.; Dimitrakopoulos, C. D.; Gelorme, J. D.; Kosbar, L. L.; Graham, T. O. *Appl. Phys. Lett.* **2002**, *80*, 2517−2519.
(8) Pesavento, P. V.; Chesterfield, R. J.; Newman, C. R.; Frisbie, C. D. *J. Appl. Phys.* **2004**, *96*, 73127324.
(9) Camerman, A.; Trotter, J. *Proc. R. Soc. London, A* **1964**, *279*, 129−146.
(10) Tang, C. W. *Appl. Phys. Lett.* **1986**, *48*, 183−185.
(11) Tan, L.; Curtis, M. D.; Francis, A. H. *Chem. Mater.* **2003**, *15*, 2272−2279.
(12) Bu, L.; Guo, X.; Yu, Bo; Qu, Y.; Xie, Z.; Yan, D.; Geng, Y.; Wang, F. *J. Am. Chem. Soc.* **2009**, *131*, 13242−13243.
(13) Zhang, Q.; Cirpan, A.; Russell, T. P.; Emrick, T. *Macromolecules* **2009**, *42*, 1079−1082.
(14) Rajaram, S.; Armstrong, P. B.; Kim, B. J.; Frechet, J. M. J. *Chem. Mater.* **2009**, *21*, 1775−1777.
(15) Mikroyannidis, J. A.; Stylianakis, M. M.; Sharma, G. D.; Balraju, P.; Roy, M. S. *J. Phys. Chem. C* **2009**, *113*, 7904−7912.
(16) Weaver, J. E.; Dasari, M. R.; Datar, A.; Talapatra, S.; Kohli, P. *ACS Nano* **2010**, *4*, 6883−6893.
(17) Cappel, U. B.; Karlsson, M. H.; Pschirer, N. G.; Eickemeyer, F.; Schoneboom, J.; Erk, P.; Boschloo, G.; Hagfeldt, A. *J. Phys. Chem. C* **2009**, *113*, 14595−14597.
(18) Cho, K J.; Shim, H. K.; Kim, Y. I. *Synth. Met.* **2001**, *117*, 153−155.
(19) Marcon, R. O.; dos Santos, J. G.; Figueiredo, K. M.; Brochsztain, S. *Langmuir* **2006**, *22*, 1680−1687.
(20) Zhao, L.; Ma, T.; Bai, H.; Lu, G.; Li, C.; Shi, G. *Langmuir* **2008**, *24*, 4380−4387.
(21) Lee, W.; Kang, S. H.; Min, S. K.; Sung, Y. E.; Han, S. H. *Electrochem. Commun.* **2008**, *10*, 1579−1582.
(22) Diguna, L. J.; Shen, Q.; Kobayashi, J.; Toyoda, T. *Appl. Phys. Lett.* **2007**, *91*, 2311623118.
(23) Lee, Y. L.; Huang, B. M.; Chien, H. T. *Chem. Mater.* **2008**, *20*, 6903−6905.
(24) Wonneberger, H.; Pschirer, N.; Bruder, I.; Schoeneboom, J.; Ma, C. Q.; Erk, P.; Li, C.; Baeuerle, P.; Muellen, K. *Chem. Asian J.* **2011**, *6*, 1744−1747.
(25) Kowerbo, D.; Schuster, J.; Amecke, N.; Abdel-Mottaleb, M.; Dobrawa, R.; Würthner, F.; von Borczyskowski, C *Phys. Chem. Chem. Phys.* **2010**, *12*, 4112−4123.
(26) Wang, C.; Huang, Z.; Bai, X.; Huang, N.; Wang, B. *Pigm. Resin Technol.* **2006**, *35*, 132−136.
(27) Vercelli, B.; Zotti, G.; Berlin, A.; Pasini, M.; Natali, M. *J. Mater. Chem.* **2011**, *21*, 8645−8652.
(28) Zotti, G.; Vercelli, B.; Berlin, A.; Chin, P. T. K.; Giovanella, U. *Chem. Mater.* **2009**, *21*, 2258−2271.
(29) Zotti, G.; Vercelli, B.; Berlin, A.; Pasini, M.; Nelson, T. L.; McCullough, R. D.; Virgili, T. *Chem. Mater.* **2010**, *22*, 1521−1532.
(30) Yu, W. W.; Qu, L.; Guo, W.; Peng, X. *Chem. Mater.* **2003**, *15*, 2854−2860.
(31) Wang, C. J.; Shim, M.; Guyot-Sionnest, P. *Science* **2001**, *291*, 2390−2392.
(32) Wang, W.; Zhai, J.; Jiang, L.; Bai, F.; Ren, Y.; Zhang, B.; Cai, S. *Colloids Surf., A* **2005**, *257−258*, 489−495.
(33) Weiss, D.; Kietzmann, R.; Mahrt, J.; Tufts, B.; Storck, W.; Willig, F. *J. Phys. Chem.* **1992**, *96*, 5320−5325.
(34) Bube, R. H. *Photoconductivity of Solids*; Wiley: New York, 1960.
(35) Murphy, A. R.; Frechet, J. M. *Chem. Rev.* **2007**, *107*, 1066−1096.
(36) Coropceanu, V.; Cornil, J.; da Silva Filho, D. A.; Olivier, Y.; Silbey, R.; Bredas, J .L. *Chem. Rev.* **2007**, *107*, 926−952.
(37) Nasr, C.; Hotchandani, S.; Kamat, P. V. *J. Phys. Chem. B* **1998**, *102*, 4944−4951.
(38) Gratzel, M. *Pure Appl. Chem.* **2001**, *73*, 459−467.
(39) Kamat, P. V. *J. Phys. Chem. C* **2008**, *112*, 18737−18753.